

## Dynamics of dry granular avalanches

Raphaël Fischer,<sup>1</sup> Philippe Gondret,<sup>1</sup> Bernard Perrin,<sup>2</sup> and Marc Rabaud<sup>1</sup><sup>1</sup>Lab FAST, CNRS, Université Pierre et Marie Curie-Paris 6, Université Paris-Sud, Bâtiment 502, Campus Universitaire, F-91405 Orsay cedex, France<sup>2</sup>LPA, CNRS, Ecole Normale Supérieure, Université Pierre et Marie Curie-Paris 6, Université Denis Diderot-Paris 7, 24 rue Lhomond, 75231 Paris cedex, France

(Received 11 May 2007; published 5 August 2008)

A fine analysis of the statistics of dry granular avalanches in a rotating drum setup reveals that, beyond the fluctuations, the angle at which an avalanche ends is correlated experimentally to the angle at which the avalanche starts. This correlation resulting from inertia defines an intermediate “neutral” angle that characterizes the corresponding granular pile. In addition, an intensive study of the dynamics of the avalanche shows that the time duration of the avalanche is correlated to its amplitude, being smaller for higher amplitude. The time relaxation of the pile slope during any avalanche, governed by the deviation of the starting angle from the neutral angle, follows a master curve. A simple model recovers most of the results and contributes to a better understanding of the physics of the avalanche flow.

DOI: [10.1103/PhysRevE.78.021302](https://doi.org/10.1103/PhysRevE.78.021302)

PACS number(s): 45.70.Ht

Granular matter has been extensively studied by physicists for about two decades, especially the granular flows in different geometries—chute flows, rotating drums, inclined planes, confined piles, shear cells—searching for the granular rheology [1] with the unknown internal stresses of collisional or frictional origin. A better knowledge of granular flows is crucial in numerous natural or industrial situations (debris flows, snow avalanches, powder handling, etc.). Despite important progress, the mechanisms that make a pile relaxing by a sudden superficial avalanche flow from the starting angle  $\theta_m$  down to the stopping angle  $\theta_r$  are not yet well understood. It is known that there is experimentally a typical finite value of avalanche amplitude  $\Delta\theta = \theta_m - \theta_r$  [2], except if the pile is too small which leads to a power law distribution without any typical value [3]. The avalanche amplitude is known to exhibit large fluctuations of order  $1^\circ$  around a mean value of about few degrees, with a Gaussian-like distribution [2,4]. Both characteristic angles  $\theta_m$  and  $\theta_r$  have also been found to fluctuate around a mean value, with smaller fluctuations for  $\theta_r$  than for  $\theta_m$ . If the starting angle  $\theta_m$  has essentially a geometrical origin [5] with a slight influence of solid friction or adhesion, except for high humidity level [6], the origin of the stopping angle  $\theta_r$  is less clear. A third angle arises from theoretical ideas: The concept of a dynamic or neutral angle which can be different from the angle of repose  $\theta_r$  indeed emerged progressively [4,7–10]. This angle is introduced either as corresponding to the dynamic friction coefficient  $\mu_d = \tan \theta_d$  at low velocities [4,8] or as the angle  $\theta_n$  for which the process of grain accretion compensates exactly the process of grain erosion [9,10]. This angle  $\theta_n$  was measured only in an inclined open box experiment [11]. Concerning the time duration of avalanches, if some theoretical studies [9,10] lead to some predictions, the few experimental studies [2,12] do not mention any dependence of the duration of avalanches with their amplitude. Furthermore, no experimental work concerns the detailed time relaxation of a pile slope except for situations very far from equilibrium [13–16].

In this paper, we focus on the relaxation dynamics of natural granular avalanches. The experimental setup is a ro-

tating cylinder of diameter  $2R$  ranging from 8 to 50 cm and width  $b$  ranging from 2 to 10 cm. The drum is half filled with monodisperse glass beads of diameter  $d$  ranging from 0.2 to 8 mm. By a classical video camera ( $750 \times 500$  pixels, 50 images/s), the entire pile is recorded and the interface is tracked by image analysis so as to measure its instantaneous mean slope angle  $\theta(t)$  with a typical resolution of  $0.01^\circ$ . The drum is rotating slowly enough to be in the regime of discrete avalanches: A quick avalanche flow lasting typically 1 s arises after typically 1 min of solid rotation at the drum angular velocity  $\Omega \approx 0.02^\circ/\text{s}$ , so that the typical time evolution of the pile slope is the one of Fig. 1. Note that in this regime of natural avalanches, the interface remains flat during the avalanche flow and that no up or down fronts are observed. The measurement of the mean slope angle  $\theta(t)$  of the pile thus remains pertinent at any time. The starting angle  $\theta_m$  (respectively the stopping angle  $\theta_r$ ) appears as the up (respectively down) tips in the “saw tooth” plot of Fig. 1, fluctuating around the value  $25^\circ$  (respectively  $23.5^\circ$ ) with thus an avalanche amplitude  $\Delta\theta$  around  $1.5^\circ$ .

The fluctuations of  $\theta_m$ ,  $\theta_r$ , and  $\Delta\theta$  analyzed for a set of 340 successive avalanches can be seen in Fig. 2. The corresponding histograms display bell shapes with the corresponding mean values and standard deviation:  $\theta_m = 25.1^\circ \pm 0.3^\circ$ ,  $\theta_r = 23.4^\circ \pm 0.15^\circ$ , and  $\Delta\theta = 1.65^\circ \pm 0.35^\circ$ . The  $\theta_m$  and  $\theta_r$  values are close but their distributions do not

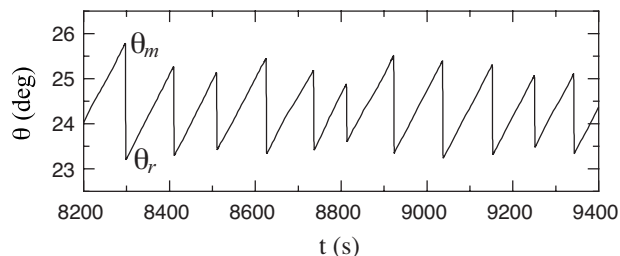


FIG. 1. Time evolution of the pile slope  $\theta$  for glass beads of diameter  $d=1$  mm in a drum of diameter  $2R=50$  cm and width  $b=5$  cm rotating at the angular velocity  $\Omega \approx 0.018^\circ/\text{s}$ .

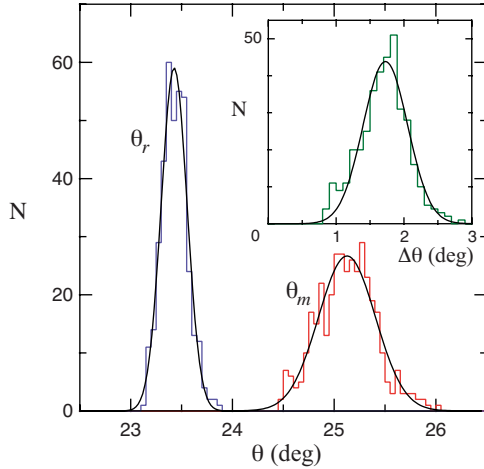


FIG. 2. (Color online) Histograms of  $\theta_m$  and  $\theta_r$ , and of  $\Delta\theta$  in inset, for 340 avalanches of glass beads ( $d=1$  mm) in a rotating drum ( $2R=50$  cm,  $b=5$  cm). (—) Best Gaussian fits.

overlap and no avalanches of amplitude below  $0.8^\circ$  have been recorded.

When the stopping angle  $\theta_r$  of any avalanche is plotted as a function of the corresponding starting angle  $\theta_m$ , it appears a weak but unambiguous correlation of negative slope coefficient: Despite large fluctuations, avalanches that start at a high angle tend to stop at a low angle (Fig. 3). By this correlation, one can define a “neutral” angle that would be the angle of zero avalanche amplitude. This neutral angle  $\theta_n = 23.7^\circ \pm 0.15^\circ$  is significantly below the average angle  $(\theta_m + \theta_r)/2$  and above the mean stopping angle  $\theta_r$ . As the slope coefficient of the correlation is  $-0.22$ , the mean neutral angle is  $\theta_n = \theta_r + 0.18\Delta\theta$ .

Let us now examine how precisely the slope interface relaxes in time from  $\theta_m$  to  $\theta_r$ . Figure 4 shows two typical relaxation curves  $\theta(t)$  for two different values of the starting angle  $\theta_m$ : We see that the avalanche which starts at a larger angle  $\theta_m$  stops at a smaller angle  $\theta_r$  (as already seen statisti-

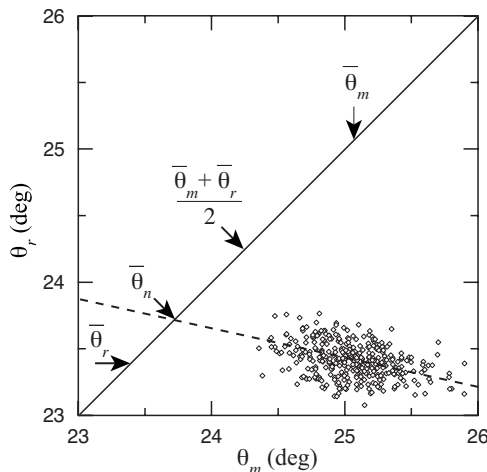


FIG. 3. Stopping angle  $\theta_r$  as a function of the starting angle  $\theta_m$  for each of the 340 avalanches of Fig. 2. ( $\diamond$ ) Experimental results and (---) best linear fit of slope  $-0.22$  and intercept  $\theta_n \approx 23.7^\circ$  with the bisector  $\theta_r = \theta_m$ .

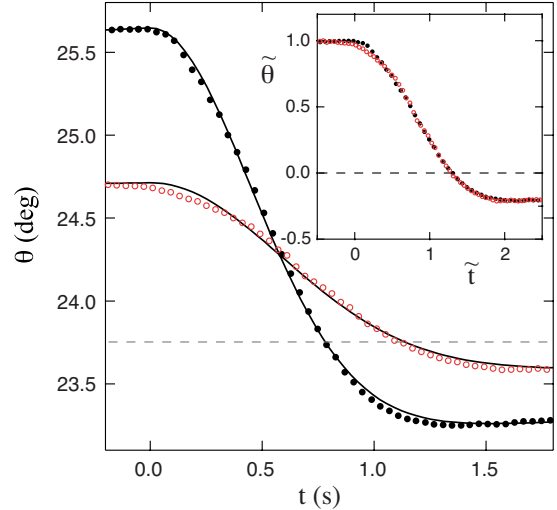


FIG. 4. (Color online) Experimental time evolution of  $\theta$  for two avalanches ( $\bullet$ ,  $\circ$ ) of different amplitudes  $\Delta\theta$ , together with the corresponding Gaussian fits (—): ( $\bullet$ )  $\theta_m=25.64^\circ$ ,  $\theta_r=23.25^\circ$ , and  $\tau=0.64$  s ( $\theta_n=23.68^\circ$ ); ( $\circ$ )  $\theta_m=24.71^\circ$ ,  $\theta_r=23.59^\circ$ , and  $\tau=0.83$  s ( $\theta_n=23.79^\circ$ ). The dashed line corresponds to the neutral angle  $\theta_n \approx 23.74^\circ$ . Inset: same data in the normalized plot [ $\tilde{\theta}=(\theta-\theta_n)/(\theta_m-\theta_n)$ ,  $\tilde{t}=t/\tau$ ].

cally in Fig. 3) in a shorter time (the neutral angle  $\theta_n$  is indeed crossed after  $\sim 0.8$  s instead of  $\sim 1.1$  s for the smaller avalanche). By fitting these relaxation curves by Gaussians of the form  $\theta(t) = \theta_r + \Delta\theta \exp(-t^2/\tau^2)$  we find a characteristic time  $\tau$  for each avalanche. The inset of Fig. 4 shows the same data in a normalized plot where the reduced deviation of the slope angle from the neutral angle,  $\tilde{\theta} = (\theta - \theta_n)/(\theta_m - \theta_n)$ , is displayed as a function of the nondimensional time  $\tilde{t} = t/\tau$ . The normalized curves corresponding to the two avalanches collapse onto a single curve close to the Gaussian curve  $\tilde{\theta} = -0.22 + 1.22 \exp(-\tilde{t}^2)$ . Note that we define for each avalanche a neutral angle by  $\theta_n = \theta_r + 0.18\Delta\theta$  as we believe that  $\theta_n$  also fluctuates with the slightly different configurations explored by the pile. By processing the 340 avalanches in the same way, we obtain the normalized plot of Fig. 5 where the solid line stands for the mean value whereas the two dotted lines stand for the corresponding standard deviation. One can see that the dispersion is rather weak meaning that a unique curve exists for the time relaxation of the slope angle when expressed in the appropriate reduced parameters.

The precise determination of the time scale  $\tau$  of each avalanche shows that  $\tau$  is correlated to the avalanche amplitude  $\Delta\theta$ ,  $\tau$  being smaller for larger  $\Delta\theta$  (Fig. 6). The detailed analysis of such a dependence  $\tau$  vs  $\Delta\theta$  has been achieved by doing experiments with different grain diameters ( $0.2 < d < 8$  mm), drum radii ( $4 < R < 25$  cm,  $30 < R/d < 350$ ), and widths ( $2 < b < 10$  cm,  $10 < b/d < 100$ ,  $0.1 < b/R < 0.5$ ). The results show that  $\tau$  does not vary with  $d$  nor with  $b$  (except via the possible  $\Delta\theta$  variation) but scales as  $(R/g\Delta\theta)^{1/2}$  (Fig. 6 and inset). This result will be discussed later.

Let us now present a simple model for the avalanche dynamics which reproduces our main experimental findings: (i) the stopping angle  $\theta_r$  is correlated to the starting angle  $\theta_m$  via

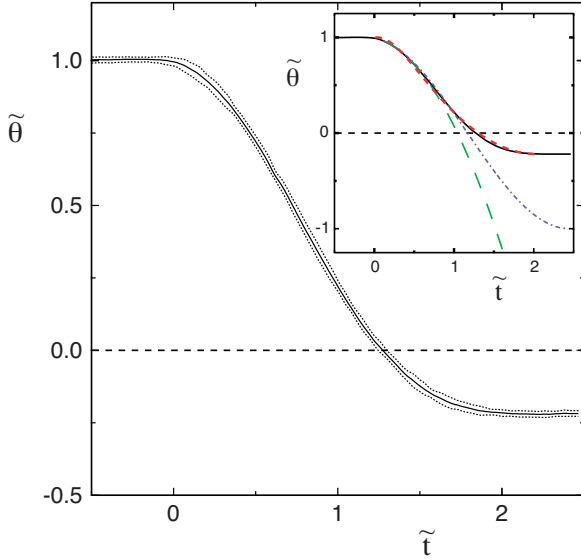


FIG. 5. (Color online) Normalized time evolution of the reduced pile angle for the 340 avalanches: Experimental average time evolution (—) and standard deviation ( $\cdots$ ). Inset: Same data (—) with the “free fall” parabolic approximation (---), the cosine “collisionless” approximation (— · —) and the adjusted solution from complete model equation (4) (—).

an intermediate “neutral” angle  $\theta_n$ , (ii) the time relaxation of the pile slope is asymmetric with respect to  $\theta_n$ , with a shape close to half a Gaussian curve, and (iii) the time duration  $\tau$  of each avalanche is correlated to its amplitude  $\Delta\theta$  (thus to the initial deviation  $\theta_m - \theta_n \approx 0.82\Delta\theta$ ) with the scaling  $\tau \sim (R/g\Delta\theta)^{1/2}$ .

Considering a thin layer of grains of thickness  $\lambda$  in motion with the velocity  $v(t)$  at the pile surface of slope  $\theta$ , the slope variation  $\dot{\theta}(t)$  is related to  $v(t)$  by mass conservation as the grain flux  $q(t)$  per unit width at the drum center is  $q(t) = \lambda v(t) = -(R^2/2)(d\theta/dt)$ . The time dynamics of the pile slope can then be written by momentum conservation as

$$dv/dt = -(R^2/2\lambda)(d^2\theta/dt^2) = g(\sin\theta - \mu \cos\theta), \quad (1)$$

where the acceleration of the layer is the result of its tangential driving gravity force reduced by a resisting friction force. In this model, the dynamic friction coefficient  $\mu(v)$  accounts for all the complex grain interactions, i.e., trapping, solid friction, and collisions [17], and can be written as  $\mu(v) = \mu_0 + f(v)$ . The first term  $\mu_0$  is the friction coefficient at vanishing velocity which comes essentially from the trapping effect, and we will see that it corresponds to the neutral angle  $\theta_n$ :  $\mu_0 = \tan\theta_n$ . The second term is a positive function  $f(v)$  that stands for the increase of the effective friction with velocity mainly due to collisional effects. Equation (1) can then be written

$$dv/dt = g \sin(\theta - \theta_n)/\cos\theta_n - gf(v)\cos\theta. \quad (2)$$

At the very beginning of the avalanche,  $\theta(t) \sim \theta_m$  and  $f(v) \sim 0$  so that the dynamics reduces to a free fall not with the usual acting gravity  $g \sin\theta_m$  but with the effective reduced gravity  $g^* = g \sin(\theta_m - \theta_n)/\cos\theta_n \sim g\Delta\theta$ . Similar dynamics

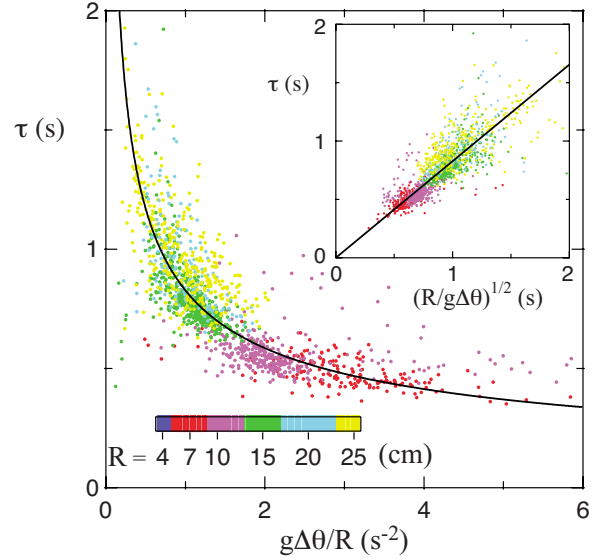


FIG. 6. (Color online) Avalanche time duration  $\tau$  as a function of  $g\Delta\theta/R$  for 1500 avalanches. Each data point corresponds to one avalanche and the different colors correspond to different drum radius  $R$  from 4 to 25 cm as indicated in the gray range. Inset: Same data as a function of  $(R/g\Delta\theta)^{1/2}$ . (—): Best fit by equation  $\tau = 0.83(R/g\Delta\theta)^{1/2}$ .

would be obtained for a mass sliding with constant friction on an inclined plane. Let us note that the experimental law for the time duration of avalanches  $\tau \approx 0.83(R/g\Delta\theta)^{1/2}$  translates exactly this free fall dynamics on the characteristic distance  $\sim R$ . The experimental curves being fitted by the Gaussian law  $\theta(t) = \theta_r + \Delta\theta \exp(-t^2/\tau^2)$ , the initial acceleration is  $(d^2\theta/dt^2)_{t=0} = -2\Delta\theta/\tau^2$ . Matching this value with the model value  $-g^*(2\lambda/R^2)$  imposes  $\lambda = \alpha R\Delta\theta$  with  $\alpha \approx 1.6$  for the flowing thickness. Let us now describe the entire dynamics. As  $\theta(t) - \theta_n$  remains always small, Eqs. (1) and (2) can be written for the reduced angle  $\tilde{\theta}$  as

$$d^2\tilde{\theta}/dt^2 + \omega^2\tilde{\theta} = \beta f(v), \quad (3)$$

with  $\omega^2 = 2\alpha g\Delta\theta/R \cos\theta_n$  and  $\beta = 2\alpha g \cos\theta_n/0.82R$ . If the  $f(v)$  term is neglected, the pile slope dynamics reduces to a cosine relaxation of period  $2\pi/\omega$  depending on the starting angle, and centered on  $\theta_n$  as the dynamics for  $\theta$  is dissipative via the nonzero friction term  $\mu_0$  ( $\theta_n \neq 0$ ). An harmonic equation has been already derived, e.g., from theoretical models [9,10] modified from Ref. [7] considering a time evolving thickness  $\lambda(t)$  and a constant downhill velocity  $v$ . The opposite is observed experimentally [18]:  $v(t)$  evolves in time with a constant  $\lambda$  that controls the exponential decrease of the velocity with the depth, which justifies the present modeling approach. The cosine solution, as the free fall parabolic approximation, deviates clearly for  $t \geq \tau$  from the experimental curve (see inset of Fig. 5) meaning that the  $f(v)$  term cannot be then neglected. Assuming for  $f(v)$  a general power law dependence  $f(v) = \gamma|v|^n$  and taking into account the existence of an experimental master curve for the pile slope relaxation  $\tilde{\theta}(\tilde{t})$ , Eq. (3) becomes

$$d^2\tilde{\theta}/d\tilde{t}^2 + A\tilde{\theta} = B(d\tilde{\theta}/d\tilde{t})^2, \quad (4)$$

with  $A = \omega^2 \tau^2 \approx 1.5\alpha$  and  $B = R/L$ , where  $L \approx 2.7\alpha/\gamma g$  can be considered as a dissipative length for the kinetic energy [19]. Note that the quadratic dependence we find for  $f(v)$  [see Eq. (4)] was already used in Ref. [8], and is consistent with experimental results on the elementary process of grain motion [17] and with the recent modeling of the solid-liquid transition exhibited by granular matter [20]. In Eq. (4), the larger  $B$  is, the larger is the curve asymmetry with respect to  $\theta_n$ . The slope dynamics given by the complete model equation (4) is found close to the experimental slope relaxation for  $A \approx 3.6$  and  $B \approx 2.2$  (see inset of Fig. 5), which corresponds to  $\lambda \approx 2.4R\Delta\theta$  and  $L \approx 0.45R$ . This dissipative length  $L$ , equal to a fraction of the pile length, is consistent with the observed typical displacements of surface grains during the avalanche. The fact that the flowing thickness must be  $\lambda \sim R\Delta\theta$  to fit the experimental time duration agrees with the scaling arguments of mass conservation suggested by Ref. [21]. However, this prediction should be tested experimentally in detail by varying carefully the different parameters as

it is hard to conclude whether or not the first direct measurements of  $\lambda$  in Ref. [18] support such a scaling.

To conclude, we have shown that the fluctuating stopping angle is correlated to the fluctuating starting angle, via an intermediate neutral angle, characteristic of the dry granular pile in its container. This neutral angle, corresponding to the exact balance between grain erosion and grain accretion, corresponds also to the value of the effective dynamic friction coefficient of the granular pile at vanishing velocity. The correlation with smaller stopping angles for larger starting angles demonstrates the role of inertia in a closed box, in contrast to submarine avalanches which are totally dissipative and relax in a quasistatic way [22]. For the dry granular avalanches, the deviation of the starting angle from the neutral angle governs the subsequent relaxation dynamics beyond the large fluctuations inherent to granular matter. Finally, the nontrivial results that the avalanche time duration is smaller for larger avalanche amplitude arises from the existence of both inertia and solid friction.

We acknowledge D. Lhuillier, P.-Y. Lagr e, G.-M. Homsy, and E. Trizac for their fruitful comments.

- 
- [1] G. D. R. Midi, *Eur. Phys. J. E* **14**, 341 (2004).  
 [2] P. Evesque and J. Rajchenbach, *C. R. Acad. Sci., Ser. II: Mec., Phys., Chim., Sci. Terre Univers* **307**, 223 (1988); H. M. Jaeger, C.-H. Liu, and S. R. Nagel, *Phys. Rev. Lett.* **62**, 40 (1989).  
 [3] G. A. Held, D. H. Solina, D. T. Keane, W. J. Haag, P. M. Horn, and G. Grinstein, *Phys. Rev. Lett.* **65**, 1120 (1990); C.-H. Liu, H. M. Jaeger, and S. R. Nagel, *Phys. Rev. A* **43**, 7091 (1991).  
 [4] M. Caponeri, S. Douady, S. Fauve, and C. Laroche, in *Mobile Particulate Systems*, edited by E. Guazzelli and L. Oger (Kluwer Academic, Dordrecht, 1995), pp. 331–336.  
 [5] R. Albert, I. Albert, D. Hornbaker, P. Schiffer, and A. L. Barabasi, *Phys. Rev. E* **56**, R6271 (1997).  
 [6] L. Bocquet, E. Charlaix, and F. Restagno, *C. R. Phys.* **3**, 207 (2002), and references herein.  
 [7] J.-P. Bouchaud, M. E. Cates, J. Ravi-Prakash, and S. F. Edwards, *J. Phys. I* **4**, 1383 (1994).  
 [8] S. J. Linz and P. Hanggi, *Phys. Rev. E* **51**, 2538 (1995).  
 [9] T. Boutreux and P.-G. de Gennes, *C. R. Acad. Sci., Ser. IIb: Mec., Phys., Chim., Astron.* **325**, 85 (1997); **326**, 257 (1998).  
 [10] A. Aradian, E. Rapha el, and P.-G. de Gennes, *C. R. Phys.* **3**, 187 (2002), and references herein.  
 [11] D. Bideau, I. Ippolito, M. A. Aguirre, A. Calvo, and N. Nerone, in *Powders and Grains 2001*, edited by Y. Kishino (Balkema, Tokyo, 2001), pp. 459–462.  
 [12] S. Courrech du Pont, P. Gondret, B. Perrin, and M. Rabaud, *Phys. Rev. Lett.* **90**, 044301 (2003).  
 [13] A. Daerr and S. Douady, *Europhys. Lett.* **47**, 324 (1999).  
 [14] S. Siavoshi and A. Kudrolli, *Phys. Rev. E* **71**, 051302 (2005).  
 [15] E. Lajeunesse, J. B. Monnier, and G. M. Homsy, *Phys. Fluids* **17**, 103302 (2005), and references therein.  
 [16] J.-F. Boudet, Y. Amarouchene, and H. Kellay, *Phys. Rev. Lett.* **96**, 158001 (2006).  
 [17] L. Quartier, B. Andreotti, S. Douady, and A. Daerr, *Phys. Rev. E* **62**, 8299 (2000).  
 [18] S. Courrech du Pont, R. Fischer, P. Gondret, R. Fischer, B. Perrin, and M. Rabaud, *Phys. Rev. Lett.* **94**, 048003 (2005).  
 [19] H. M. Jaeger *et al.*, *Europhys. Lett.* **11**, 619 (1990).  
 [20] P. Mills, P. Rognon, and F. Chevoir, *Europhys. Lett.* **81**, 64005 (2008).  
 [21] J. Rajchenbach, *Adv. Phys.* **49**, 229 (2000).  
 [22] D. Doppler, P. Gondret, T. Loiseleux, S. Meyer, and M. Rabaud, *J. Fluid Mech.* **577**, 161 (2007).